MOLECULAR AND SYNAPTIC MECHANISMS

Novel fast adapting interneurons mediate cholinergic-induced fast GABA$_A$ inhibitory postsynaptic currents in striatal spiny neurons

Thomas W. Faust, Maxime Assous, Fulva Shah, James M. Tepper and Tibor Koós
Center for Molecular and Behavioral Neuroscience, Rutgers, the State University of New Jersey, 197 University Avenue, Newark, NJ 07102, USA

Abstract

Previous work suggests that neostriatal cholinergic interneurons control the activity of several classes of GABAergic interneurons through fast nicotinic receptor-mediated synaptic inputs. Although indirect evidence has suggested the existence of several classes of interneurons controlled by this mechanism, only one such cell type, the neuropeptide-Y-expressing neurogliaform neuron, has been identified to date. Here we tested the hypothesis that in addition to the neurogliaform neurons that elicit slow GABAergic inhibitory responses, another interneuron type exists in the striatum that receives strong nicotinic cholinergic input and elicits conventional fast GABAergic synaptic responses in projection neurons. We obtained *in vitro* slice recordings from double transgenic mice in which Channelrhodopsin-2 was natively expressed in cholinergic neurons and a population of serotonin receptor-3a-Cre-expressing GABAergic interneurons were visualized with tdTomato. We show that among the targeted GABAergic interneurons a novel type of interneuron, termed the fast-adapting interneuron, can be identified that is distinct from previously known interneurons based on immunocytochemical and electrophysiological criteria. We show using optogenetic activation of cholinergic inputs that fast-adapting interneurons receive a powerful supra-threshold nicotinic cholinergic input *in vitro*. Moreover, fast adapting neurons are densely connected to projection neurons and elicit fast, GABA$_A$ receptor-mediated inhibitory postsynaptic current responses. The nicotinic receptor-mediated activation of fast-adapting interneurons may constitute an important mechanism through which cholinergic interneurons control the activity of projection neurons and perhaps the plasticity of their synaptic inputs when animals encounter reinforcing or otherwise salient stimuli.

Introduction

The recent introduction of transgenic reporter methods into the study of striatal circuits has not only led to the discovery of several new classes of striatal GABAergic interneurons but also revealed important and unexpected features of their circuit organization. Of particular interest, direct and indirect evidence now indicates that a subset of GABAergic interneurons receives a powerful nicotinic excitatory synaptic input. This phenomenon, first inferred from evidence showing recurrent inhibition in cholinergic interneurons (Sullivan *et al.*, 2008) and later confirmed and extended using paired recordings and optogenetics (English *et al.*, 2012), suggests that contrary to the prevailing view some striatal GABAergic interneurons may not be driven exclusively by the cortical and thalamic inputs that they share with the main projection neuron population, but to a significant degree by intrastriatal and perhaps extrastriatal cholinergic inputs. This observation, together with the existence of feedback inhibition

of cholinergic [choline-acetyltransferase-expressing (ChAT)] interneurons and the selective electrotonic and synaptic connectivity of different GABAergic interneurons, suggests that the function of interneurons may not be limited to the currently envisaged feed-forward gating of cortical and thalamic excitation of projection neurons. Instead, the interconnected ChAT and GABAergic interneurons may transmit afferent signals that are not directly received by projection neurons and integrate them with other striatal inputs through the emergent dynamics of their circuitry. The picture of a complex and perhaps semi-autonomous network of ChAT and GABAergic interneurons provides impetus for more detailed characterization of this circuitry, with particular emphasis on the number, intrinsic properties and connectivity of neurons that receive significant nicotinic synaptic inputs. To date, only one such GABAergic interneuron, the neuropeptide-Y-expressing neurogliaform (NPY-NGF) neuron has been identified (Ibáñez-Sandoval *et al.*, 2011; English *et al.*, 2012). Indirect evidence however suggests that other interneurons may also be activated by nicotinic synaptic inputs. The existence of one of these putative interneurons was inferred from experiments where multiphasic disynaptic GABAergic inhibitory postsynaptic currents (IPSCs) were elicited in sympathetic preganglionic neurons (SPNs) with synchronous optogenetic activation of ChAT interneurons (English

et al., 2012). This study suggested that a conventional fast GAB-Aergic IPSC component of the compound response in SPNs may originate from a type of neuron that is distinct from the NPY-NGF interneuron. Alternatively, however, part or perhaps all of this inhibitory response may arise from axon terminals of extrastriatal afferent neurons that express presynaptic nicotinic receptors, as shown for dopaminergic inputs by Nelson et al. (2014). Here we tested the hypothesis that there exists a population of striatal GABAergic interneurons that mediate fast synaptic inhibition of SPNs in response to cholinergic excitatory signals.

Materials and methods

Animals

All procedures used in this study were performed in agreement with the National Institutes of Health Guide to the Care and Use of Laboratory Animals and with the approval of the Rutgers University Institutional Animal Care and Use Committee. HTR3a-Cre mice (Tg(HTR3a-Cre)NO152Gsat/Mmucd, University of Davis) (Gerfen et al. 2013), ChAT-ChR2 mice (Tg(Chat-COP4*H134R/EYFP,Slc18a3)6Gfng/J; Jackson Labs, Bar Harbor, MA, USA) and double transgenic mice (ChAT-ChR2-EYFP;HT3Ra-Cre) were generated and maintained as hemizygotic. Mice were housed in groups of up to four per cage and maintained on a 12-h light cycle (07:00–19:00 h) with ad libitum access to food and water. In total, 45 mice were used, including both males and females.

Intracerebral viral injection

Mice were injected with recombinant, replication incompetent serotype-5 Adenovirus-associated virus vector (rAAV2/5) carrying an expression cassette consisting of double-floxed, inverted open reading frame coding sequences (CDS) for ChR2-(H134R)-eYFP or tdTomato under the respective control of EF1a or CAG promoters and, downstream of the CDS, a woodchuck hepatitis post-transcriptional regulatory element (WPRE) and a human growth hormone poly-adenylation (hGA) sequence. Virus stock was obtained from the University of North Carolina Vector Core Services (Chapel Hill, NC, USA). The surgery and viral injection took place inside a Biosafety Level-2 isolation hood. Mice were anesthetized with isofluorane (1.5–3%, delivered with O_2, 1 L/min) and placed within a stereotaxic frame. A single dose of enrofloxacin (Baytril), 10 mg/kg, s.c., was given to prevent infections. Bupivacaine was used as a local anesthetic at the site of surgery. A single craniotomy was made at coordinates +0.74 mm anterior and 1.6–1.8 mm lateral to Bregma. Then, 0.6 μL of virus suspension (> 10^{13} viral genomes/mL titer) was delivered by glass pipette to three sites −1.75, −2.25 and −3.6 mm ventral to the brain surface, for a total volume of 1.8 μL. Virus was injected at 0.92 nL/s, after which the pipette was left in place for 10 min before being slowly retracted. During postsurgical recovery mice were kept under Biosafety level-2 confinement for 5 days and analgesia was provided for the first 3 days with 0.1 mg/kg buprenorphine, s.c. (at every 12 h) and ketoprofen s.c. (5 mg/kg daily). Expression of viral transgene was allowed for at least 2 weeks before animals were used for experiments.

Immunocytochemistry

Mice were deeply anesthetized with 150/25 mg/kg ketamine/xylazine, i.p. Brain tissue was fixed by transcardial perfusion of 10 mL of ice-cold artificial cerebrospinal fluid (adjusted to pH 7.2–7.4), followed by perfusion of 90–100 mL of 4% (w/v) paraformaldehyde, 15% (v/v) picric acid in phosphate buffer. Brains were post-fixed overnight in the same fixative solution. Sections 50–60 μm thick were cut on a Vibratome 3000. Sections were cleaned with 10% (v/v) methanol, 3% (v/v) hydrogen peroxide in phosphate-buffered saline (PBS), followed by 1% (w/v) sodium borohydride in PBS. Sections were blocked in 10% (v/v) normal donkey serum, 3% (w/v) bovine serum albumin and 0.5% (v/v) Triton X-100 in PBS overnight at 4 °C. Alternating serial sections were incubated for 24 h at room temperature in the following primary antibodies and at the following concentrations: rabbit anti-parvalbumin (PV) (catalog #24428; Immunostar, Hudson, WI, USA) 1 : 1500, rabbit anti-calretinin (CR) (catalog #24445; Immunostar) 1 : 1500, goat anti-nitric oxide synthase (NOS) (catalog #Ab1376; Abcam, Cambridge, MA, USA) 1 : 1000, rabbit anti-neuropeptide-Y (NPY) (catalog #Ab30914; Abcam). Sections were incubated in the following secondary antibodies, raised in donkey, overnight at 4 °C: 1 : 400 (NOS) anti-goat Alexa Fluor© 594 (catalog #A-11058; Life Technologies, Carlsbad, CA, USA), 1 : 400 (PV, CR) anti-rabbit Alexa Fluor© 594 (catalog #A-11032; Life Technologies) and 1 : 500 (NPY) anti-rabbit Alexa Fluor© 594. In one case where tdTomato virus was injected, the tissue was processed in 1 : 1500 rabbit anti-tyrosine hydroxylase (TH) (catalog #ab152; Millipore, Billerica, MA, USA) primary antibody and its respective 1 : 300 donkey anti-rabbit Alexa Fluor© 488 (catalog #A-21206; Life Technologies) secondary antibody. Immunocytochemical detection of TH in striatal interneurons requires prior 6-OHDA-mediated lesioning of the nigrostriatal dopaminergic projection, which was conducted as described by Ünal et al. (2013). Sections were mounted in Vectashield (Vector Labs, Burlingame, CA, USA).

Slice preparation and visualized in vitro whole cell recording

Mice aged 3–7 months were deeply anesthetized with 150/25 mg/kg ketamine/xylazine, i.p., prior to surgery. Acute brain slices were prepared as previously described (Tecuapetla et al., 2009), with the following exceptions. Mice were transcardially perfused with ice cold or partially frozen N-methyl-D-glucamine (NMDG)-based solution consisting of following (in mM): 103.0 NMDG, 2.5 KCl, 1.2 NaH_2PO_4, 30.0 $NaHCO_3$, 20.0 HEPES, 25.0 glucose, 101.0 HCl, 10.0 $MgSO_4$, 2.0 thiourea, 3.0 sodium pyruvate, 12.0 N-acetyl cysteine, 0.5 $CaCl_2$ (saturated with 95% O_2/5% CO_2, measured to be 300–310 mOsm and 7.2–7.4 pH). Following slice preparation, slices were allowed to recover in well-oxygenated NMDG-based solution at 35 °C for an additional 5 min, after which they were transferred to well-oxygenated normal Ringer solution at 25 °C until placed in the recording chamber constantly perfused with oxygenated Ringer solution at 32–34 °C. We recorded SPNs in voltage clamp using a CsCl-based internal solution (Tecuapetla et al., 2009). This solution also contained 0.2% (w/v) Alexa Fluor© 594, used to fill and visually verify the identity of SPNs. All other neurons were recorded with normal internal solution.

Instrumentation, voltage-clamp parameters and other aspects of fluorescence-guided visualized whole-cell recording were the same as described by Tecuapetla et al. (2009).

Optogenetic stimulation in vitro consisted of 1- to 2-ms blue light pulses (1.25 mW/mm^2) delivered from an LED coupled to a 200-μm multimode optical fiber placed at ~45 ° above the slice aiming at the recorded neurons, or by wide field illumination using a high-power (750-mW) LED (> 5 mW/mm^2 illumination intensity). Optogenetic pulses were delivered at 30- or 60-s intervals.

For the testing of synaptic transmission, 50-Hz trains (10 spikes) were elicited in the presynaptic cell with short current pulses. Trains were delivered at 30-s intervals.

Data analysis

As fast-adapting interneurons (FAIs) were recognized based on subjective classification of cells, we first used unsupervised clustering to examine if these neurons could be identified in an unbiased manner among the cells exhibiting novel characteristics. As FSIs and NPY-NGFs have been previously characterized and encountered in other transgenic lines, they were excluded from clustering analysis. These cells were positively identified based on several defining instrinsic properties such as a fast spike waveform with a single fast afterhyperpolarization (AHP) for the fast-spiking interneuron (FSI), whereas NPY-NGFs exhibited a single slow AHP. FAIs and all other unclassified cells submitted for clustering exhibited both fast and slow AHPs at or close to rheobase (see Figs 2C and D, 3B, and 5C), demonstrating their difference from the other two cell types in this example. The most salient difference between FAIs and other novel cells was that all the other novel cells rapidly entered depolarization block. To use this property for classification we chose two quantitative metrics that capture interrelated but distinct aspects of how the firing of action potentials depends on somatically injected current amplitude (Fig. 2F). The first, more straightforward one is the steepness of the current–firing frequency relationship. The second is the degree to which the cells are liable to depolarization block at higher current amplitudes. Depolarization block directly affects the total number of spikes fired during current injection in a manner that often *reduces* rather than increases the number of spikes with increasing current amplitudes above the level where depolarization block first develops. As a result the relationship between the injected current and the total number of spikes per episode is not monotonic but U-shaped and the increasing tendency for depolarization block results in an increasing deviation from a linear relationship between injected current and the number of elicited spikes. To capture quantitatively the degree of deviation from linearity we used linear regression to compute the coefficient of determination (r^2) for each cell's current spike–frequency relationship. (Note that application of the linear regression to U-shaped current–frequency relationships explains the negative slope values found for several neurons, Fig. 2F.) Next, the current–frequency relationships were transformed for each cell into a 2D vector, with one dimension representing the slope of the linear fit to the spike–frequency relationship and the second dimension corresponding to the coefficient of determination for the computed fit. These vectors are plotted in the plane of the corresponding dimensions in Fig. 2F. Next we used a K-means clustering algorithm implemented in Matlab (Mathworks, Natick, MA, USA) with the number of groups chosen to be four based on an estimation of the optimal group number by the *evalclusters* algorithm of Matlab. One group, comprising 25 neurons that followed a near linear current–frequency function (high r^2) and high, positive slope values could be isolated as a distinct cluster in this distribution. The Mahalanobis distances from each of the vectors in this group to the center of the distribution were > 17. This group corresponded to the cells subjectively classified as FAI based on their rapidly developing spike frequency adaptation.

Despite the fact that the remaining 43 neurons were clustered into three separate groups by the K-means algorithm, the majority of these cells' current–frequency functions were not linear, and therefore we considered their treatment as separate groups on this basis to be ill-conceived. More specifically, because completely different non-linear functions can yield the same r^2 value if a linear fit is forced to the data, a small difference in this metric is not a reliable indicator of electrophysiological similarity. We emphasize, however, that this is not a concern for reliable discrimination of approximately linear relationships from non-linear ones as high r^2 requires linearity. For these reasons we identified only two distinct cell groups based on the cluster analysis, the FAI and the non-FAI groups, and *post hoc* statistical comparisons was performed between these two groups as described in the text. Regression analysis and statistics were performed with Origin (Originlab, Northampton, MA, USA). Population data are expressed as mean ± SD unless otherwise indicated.

Results

To identify GABAergic interneurons that receive nicotinic synaptic inputs our strategy was to generate double transgenic mice in which ChAT neurons natively express ChR2-eYFP and different types of candidate GABAergic interneurons express Cre-recombinase, in turn to be used for selective fluorescent visualization to guide systematic screening for postsynaptic cholinergic responses. As previous experiments exclude (with the possible exception of subtypes of TH-expressing interneurons, THINs) the role of currently known GABAergic interneurons in mediating fast acetylcholine-induced GABAergic inhibition in SPNs (English *et al.*, 2012) we sought to find and test new types of striatal interneurons. To this end we created a double transgenic strain using mice in which Cre-recombinase is expressed under the control of the regulatory sequence of the 5-hydroxytryptamine receptor-3-subunit-a (HTR3a) gene. Our original choice of targeting based on HTR3a gene expression was motivated by the observation that GABAergic interneurons often colocalize HT3a receptors with nicotinic receptors in other brain areas (Sudweeks *et al.*, 2002; Lee *et al.*, 2010). Subsequently, this correlation has also been confirmed in the neostriatum (Muñoz-Manchado *et al.*, 2014).

We used immunocytochemistry and *in vitro* whole-cell recording to obtain a preliminary characterization and classification of the targeted interneurons. Currently, eight different classes of interneurons have been described in the striatum (for a review, see Tepper *et al.*, 2010). These include PV expressing fast-spiking neurons, NPY and NOS co-expressing plateau-depolarization low-threshold spiking (PLTS) interneurons (Kawaguchi, 1993), NPY-expressing (but NOS-negative) NPY-NGF neurons which give rise to slow GABAergic inhibition in projection neurons (Ibáñez-Sandoval *et al.*, 2011), four electrophysiologically distinct types of neurons termed THINs which can be identified in transgenic mice on the basis of GFP or Cre expression controlled by the regulatory sequence of the TH gene (Ibáñez-Sandoval *et al.*, 2010) and, finally, interneurons with unknown electrophysiological properties that express CR (Kawaguchi *et al.*, 1995). The existence of a class of interneurons that forms reciprocal feedback inhibitory connection with ChAT interneurons have been inferred from indirect evidence (Sullivan *et al.*, 2008) and, with the possible exception of CR+ cells, these neurons are probably distinct from all other interneurons (English *et al.*, 2012).

To characterize the HTR3a-Cre neuron population we first tested the expression of PV, NPY, NOS, CR and TH using immunocytochemistry (Fig. 1). Among the transfected Cre-expressing interneurons, a large fraction was positive for PV (190 PV-immunopositive neurons, 48 HTR3a-Cre neurons, 36 neurons colocalizing, 75% of HTR3a-Cre neurons PV positive). In contrast, small populations expressed NPY (165 NPY-immunopositive cells, 156 HTR3a-Cre

cells, five colocalized, 3.2% of Htr3a-Cre neurons NPY positive) or CR (23 CR-immunopositive cells, 86 HTR3a-Cre cells, two colocalized, 2.3% of HTR3a-Cre neurons CR positive) while none contained NOS (130 NOS-immunopositive cells, 94 HTR3a-Cre cells, 0 colocalized) or exhibited TH expression after lesioning the nigrostriatal dopaminergic input (162 TH-immunopositive cells, 152 HTR3a-Cre cells, 0 colocalized; see Materials and methods). About 20% of HTR3a-Cre–eYFP-expressing neurons did not express any of these markers (Fig. 1). In addition, we also examined the possible expression of Cre in ChAT interneurons in double transgenic *ChAT-ChR2-eYFP;HT3Ra-Cre* mice virally transfected to express dTomato from a Cre-dependent (DIO) transgene (Fig. 4A). None of the HTR3a-Cre cells expressed ChR2-eYFP, demonstrating that ChAT interneurons were not part of the HTR3a-Cre neuron population (177 ChAT-ChR2-eYFP cells, 109 HTR3a-Cre cells, 0 colocalized, Fig. 4A). Finally, the possible involvement of SPN neurons could be excluded on morphological (as well as electrophysiological, see below) grounds as none of the HTR3a-Cre neurons exhibited the high dendritic spine density or other morphological characteristics of SPNs (Fig. 1; cf. Grofova, 1974; Wilson & Groves, 1980; Somogyi *et al.*, 1981; Gertler *et al.*, 2008).

Next we obtained *in vitro* whole-cell recordings from Cre-expressing interneurons ($n = 134$). Consistent with the immunocytochemical detection of PV+ and NPY+ neurons, a large fraction of the recorded neurons were FSIs ($n = 57$, Fig. 2A) while a small population of cells exhibited the properties of NPY-NGF interneurons ($n = 5$) including a large-amplitude, long-lasting spike AHP, with long latency to the most negative point of the AHP (Fig. 2B) and as demonstrated in a subset of cells, slow GABAergic signaling to simultaneously recorded SPNs (Fig. 4E), which is the primary defining feature of NPY-NGF interneurons in the striatum (Ibáñez-Sandoval *et al.*, 2010). Consistent with our morphological observations, none of these cells exhibited the electrophysiological properties of SPNs (Fig. 2; cf. Nisenbaum *et al.*, 1994; Gertler *et al.*, 2008).

In addition to these known cell types we also found interneurons that exhibited electrophysiological properties not previously described in the neostriatum (Kawaguchi, 1993; Kawaguchi *et al.*, 1995; Gittis *et al.*, 2010; Ibáñez-Sandoval *et al.*, 2010, 2011; Tepper *et al.*, 2010; Sciamanna & Wilson, 2011). Although these neurons were electrophysiologically heterogeneous, one class of cells could be readily recognized based on the presence of pronounced spike-frequency adaptation during repetitive firing induced by injection of depolarizing current pulses (Fig. 2D). These neurons were termed FAIs. Further characteristics of FAIs include a resting membrane potential of -66.2 ± 1.2 mV, no spontaneous activity, a nearly linear sub-threshold current–voltage relationship only slightly distorted by weak time-dependent inward rectification and a moderate maximal sustained firing rate reaching < 100 Hz (Fig. 2D). To test whether FAIs represented a type of neuron distinct from the remaining novel interneurons we first used unsupervised clustering based on current–spike frequency relationships (see Materials and methods). As shown in Fig. 2E and F, this method identified distinct clusters within the recorded cell population, one of which corresponded directly to the neurons pre-classified as FAIs. To confirm statistically the validity of discriminating between FAIs and all other novel interneurons we compared several basic electrophysiological properties of FAIs and the remaining novel neurons. This revealed statistically significant differences in several parameters including the membrane time constant (FAI: $n = 25$, 22.43 ± 1.97 ms, mean $\pm$ SD, other: $n = 43$, 34.61 ± 2.42 ms, $t = 3.90$, two-sample t-test, $P < 0.001$), input resistance at rest (FAI: $n = 25$, 362.0 ± 104.8 MΩ, other: $n = 22$, 601.1 ± 226.5 MΩ, $t = 4.54$, two-sample

t-test, $P < 0.001$) and the latency of the most negative point of the spike AHP following an action potential (FAI: $n = 25$, 0.85 ± 0.23 ms median $\pm$ interquartile range (IQR), other: $n = 43$, 0.95 ± 0.36 ms median $\pm$ IQR, $U = 302$ $Z = -2.99$, Mann–Whitney test, $P < 0.003$). We did not attempt to further characterize or classify the novel neurons that were distinct from FAIs (these will be described in a manuscript now in preparation), but we note that they appeared to comprise more than one cell type, with many of them exhibiting features shared with subpopulations of THINs (see comments in Materials and methods). An example of the most frequently observed electrophysiological profile among these neurons is shown in Fig. 2C. The basic properties of fast-spiking, NPY-NGF, FAI and the unclassified group of novel interneurons are summarized in Table 1.

As preliminary recordings demonstrated that FAIs received nicotinic synaptic inputs and therefore were a candidate for participating in a disynaptic circuit to SPNs, we concentrated on characterizing the synaptic connectivity of this cell type. First, we obtained paired recordings from FAIs and SPNs to examine the postsynaptic responses elicited by these interneurons (Fig. 3). These tests were done using recordings from 14 FAIs and 22 SPNs, with six FAIs being tested with more than one (two or four) SPN each, and no SPN tested with more than one FAI. Postsynaptic responses could be observed in SPNs in 11 of the 22 tested connections, representing a one-way connectivity of 50%. The response was a fast GABA$_A$-receptor-mediated IPSC as it could be blocked by bicuculline ($n = 1$; Fig. 3C) and exhibited an average rise-time and decay-time constant of 1.46 ± 0.41 and 6.79 ± 0.83 ms, respectively. Remarkably, unlike all other inhibitory neostriatal connections in the neostriatum (Koos *et al.*, 2004; Taverna *et al.*, 2008; Tecupetla *et al.*, 2009; Gittis *et al.*, 2010) synaptic transmission from FAIs exhibited pronounced short-term facilitation (Fig. 3A, D and F). Strikingly, in some pairs the resting release probability (the probability of observing a synaptic response to the first stimulus in 50-Hz spike trains delivered at 30-s intervals) was close to zero (Fig. 3A, inset). On average the IPSC amplitude increased by a factor of 2.17 through the first three spikes (Fig. 3D and F). In some pairs use-dependent short-term depression was also observable late in the spike train (Fig. 3D). The population mean of the maximal IPSC amplitude was 16.9 ± 4.8 pA, which is significantly smaller than the unitary IPSC amplitudes recorded from FSIs (Fig. 1D, cf. Fig. 3E). Neither the short-term facilitation nor the small IPSC amplitude was an artifact of the preparation or recording methods as synaptic transmission from an FSI to an SPN exhibited typical properties including high-amplitude IPSCs and use-dependent depression (Fig. 3E and F). Normal synaptic transmission was also confirmed between four pairs of NPY-NGF interneurons and SPNs (Fig. 4E).

Next we characterized the postsynaptic responses of FAIs elicited by optogenetic activation of cholinergic inputs using double transgenic *ChAT-ChR2-eYFP;HT3aR-Cre* mice virally transfected to express tdTomato from a Cre-dependent (DIO) transgene (Fig. 4A). As ChR2 was here targeted to cholinergic neurons using a transgenic and not the virus-mediated process used previously and because ChR2 expression in this preparation is not limited to ChAT interneurons but includes all cholinergic neurons such as those recently reported to project to the striatum from the brainstem (Dautan *et al.*, 2014), we first tested if the synaptic responses of downstream circuits to optogenetic cholinergic stimulation were similar to the originally described responses (English *et al.*, 2012). Whole-cell recording from ChAT interneurons demonstrated that these cells exhibited normal electrophysiological characteristics, including low-frequency spontaneous activity (Fig. 4B) and
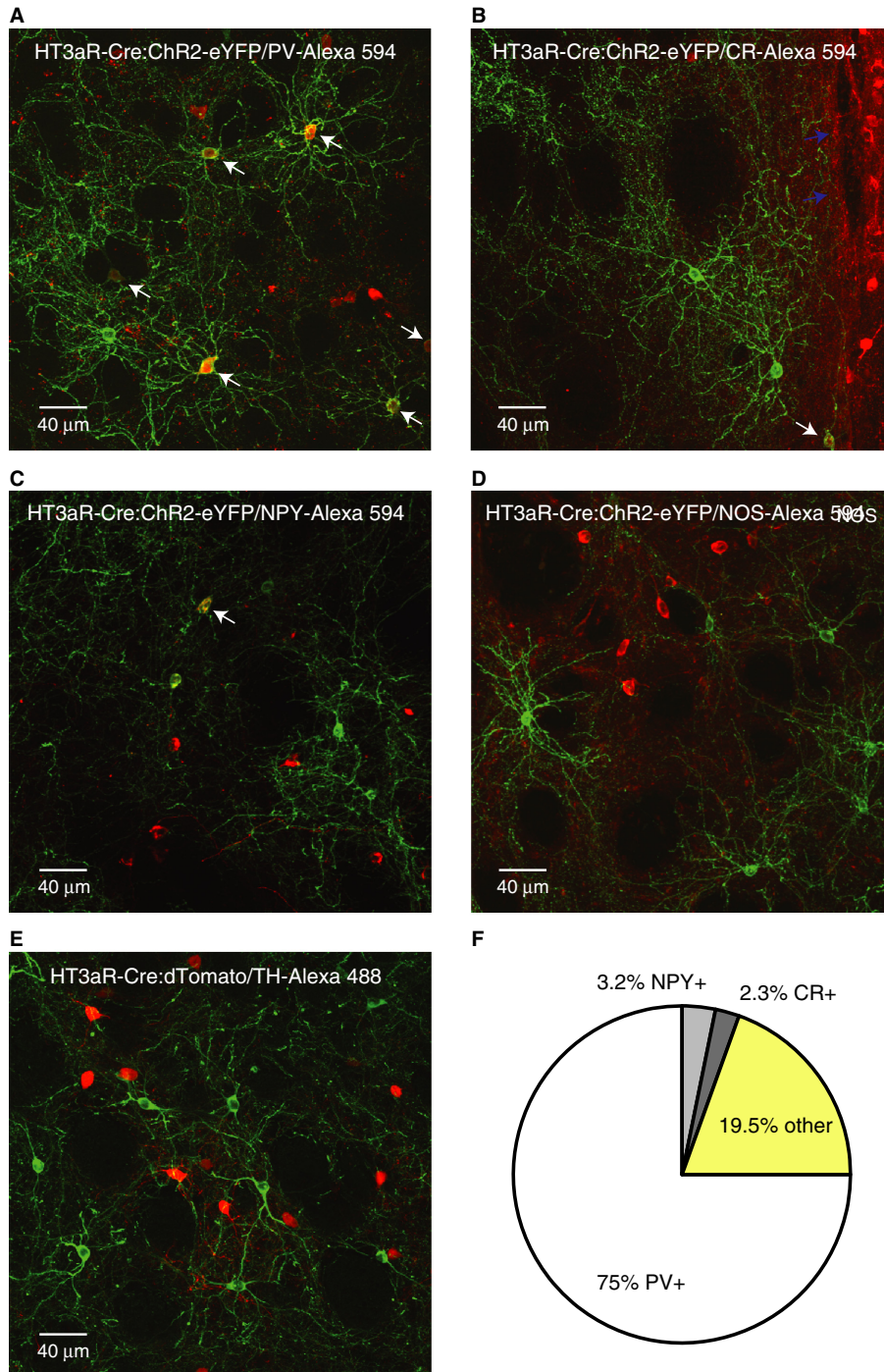
Fig. 1. Immunocytochemical characterization of HTR3a-Cre interneurons. (A–D) Confocal micrographs showing interneurons transfected with ChR2-eYFP (pseudo-colored in green) and immunolabeling visualized with Alexa-594-conjugated secondary antibodies (red) to detect the different antigens indicated in the panels. (E) Confocal micrograph showing HTR3a-Cre interneurons transfected with dTomato (red) and immunolabeling visualized with Alexa-488-conjugated secondary antibody (green) to detect TH. (A–E) White arrows point to double labeled cells wherever applicable. In B blue arrows point to the border of the lateral ventricle. (F) Quantitative summary of immunocytochemical results. Neurons labeled as *other* refer to HTR3a-Cre interneurons that were immunonegative for PV, NPY or CR, calculated on the basis that these markers are not co-expressed in the striatum.

responded with firing action potentials to pulses of blue light (1–2 ms, Fig. 4C). Consistent with previous results, optogenetic activation of ChAT interneurons elicited multiphasic IPSCs in all recorded SPNs (Fig. 4D). The IPSC comprised an early fast component and a distinct slow component, the kinetics of which was sensitive to the blockade of GABA reuptake with NO711 (10 μM,

Fig. 4D). In addition, we also recorded NPY-NGF interneurons and showed that these neurons received nicotinic excitatory postsynaptic potential (EPSPs) and elicited slow IPSCs in SPNs ($n = 3$; Fig. 4E). These results confirm that similar GABAergic circuits are activated in this preparation as in previous studies (English *et al.*, 2012; Nelson *et al.*, 2014).
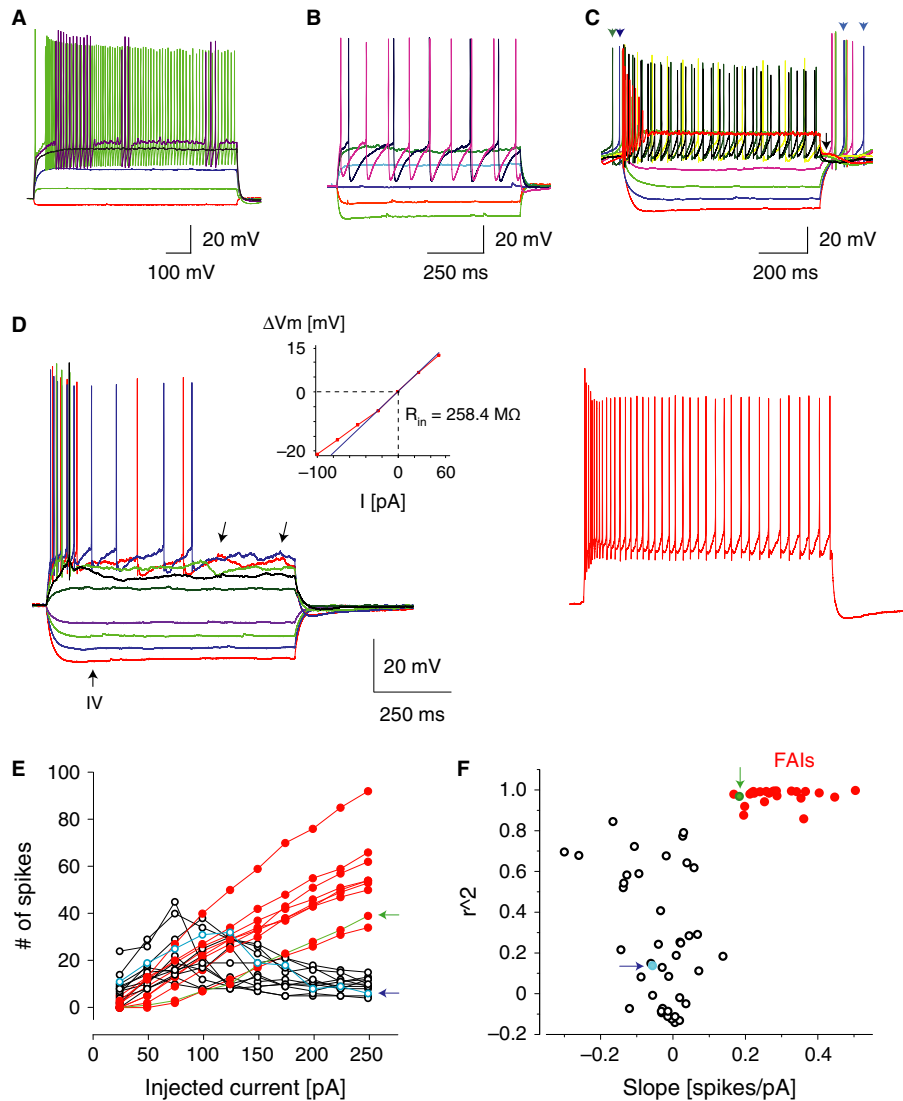
FIG. 2. Electrophysiological identification of FAIs. (A) Membrane potential responses of a typical FSI to injected current pulses. Note the distinctive 'stuttering' firing pattern and sub-threshold membrane potential oscillations. Same cell as in Fig. 3E. (B) Membrane potential responses of a typical NPY-NGF to injected current pulses. Note the large-amplitude, slow AHPs. The neuron was further identified as an NPY-NGF based on characteristic synaptic output shown in Fig. 4E. (C) Membrane potential responses of the most typical novel interneuron not classified as an FAI to injected current pulses. Same as the unclassified non-FAI cell indicated by arrows pointing to open symbols in E and F. Note the features that distinguish this neuron from FAIs, including depolarization block at high amplitudes of injected current, short-duration depolarizing plateau potential (arrow) and spontaneous activity (arrowheads). Also note the resemblance of these characteristics to those exhibited by THINs. (D) Membrane potential responses of a typical FAI to injected current pulses (25-pA steps from −100 pA, including traces in left and right panels). Same FAI as indicated by arrows pointing to closed symbols in E and F. Note the pronounced spike frequency adaptation and irregular membrane potential fluctuations (left panel, arrows). Inset shows the current–voltage relationship of this neuron. The thin line is a linear fit restricted to the current range −25 to 25 pA used to calculate slope conductance and R_{in}. Right panel shows the response of the cell to a high-amplitude current pulse (275 pA). The V_{m-rest} was −62 mV in this cell. (E and F) Cluster analysis of novel interneurons (see Materials and methods). (E) The number of action potentials fired in response to current injection is plotted as a function of the injected current amplitude for unclassified novel neurons (open symbols) and FAIs (closed symbols). Note the pronounced reduction in action potential number above a certain current amplitude in the non-classified neurons but not in FAIs. Only a subset of cells are shown for each group to avoid overcrowding. (F) Linear functions were fitted to each cell's current–frequency relationship and the coefficients of determination (r^2) were plotted as a function of the slopes of the fitted lines. Neurons pre-classified as FAIs correspond to the cluster of closed symbols. Note the clear separation of this group from the remaining novel HTR3a-Cre neurons. Arrows indicate the corresponding cells in the graphs in E and F.

Next we examined the postsynaptic responses of FAIs to optogenetic activation of cholinergic inputs (Fig. 5). In 13 of the 15 recorded FAIs (86.7%), brief light pulses (1–2 ms) elicited EPSPs exhibiting an average amplitude of 10.4 ± 6.12 mV (Fig. 5A–C). In ten of 13 cells (76.9%) the EPSP also triggered action potentials (1–3 spikes per EPSP, Fig. 5A–C). The EPSP was mediated by nicotinic acetylcholine receptors because it could be blocked by mecamylamine (MEC, 5 μM, n = 7, Fig. 5A) or the β2-subunit selective

antagonist dihydro-β-erythroidine (DHβE, 1 μM, n = 8, Fig. 5B). Interestingly, even at the relatively high concentration of 1 μM, DHβE was effective only in two FAIs (Fig. 5A and B), while in the remaining neurons the response was blocked by MEC (Fig. 5A), possibly revealing heterogeneity in nicotinic receptor subunit composition among FAIs. Successful receptor block by DHβE application in these experiments was demonstrated by the complete blockade of the disynaptic IPSC elicited in simultaneously recorded SPNs (Fig. 5A).

TABLE 1. Electrophysiological properties of HTR3a-Cre interneurons

Parameter	FSI (57)	NGF (5)	FAI (25)	Unclassified (43/22*)
Input resistance (MΩ)	84.1 ± 6.7	232.3 ± 34.8	362.0 ± 21.0	601.1 ± 48.3
Resting membrane potential (mV)	−82.0 ± 0.7	−73.1 ± 5.8	−66.2 ± 1.2	−66.1 ± 1.1
Membrane time constant (ms)	6.72 ± 0.51	14.67 ± 3.76	22.43 ± 1.97	34.61 ± 2.42
Per cent spontaneously active	0	0	0	46.5
Per cent exhibiting ADP or plateau potential	0	0	0	34.9

All values are means ± SEM.
*Only a subset of the unclassified cells (22 cells which were not spontaneously active) was used for calculating resting membrane potential and input resistance at rest. Four additional non-FAI neurons were not included in this analysis.
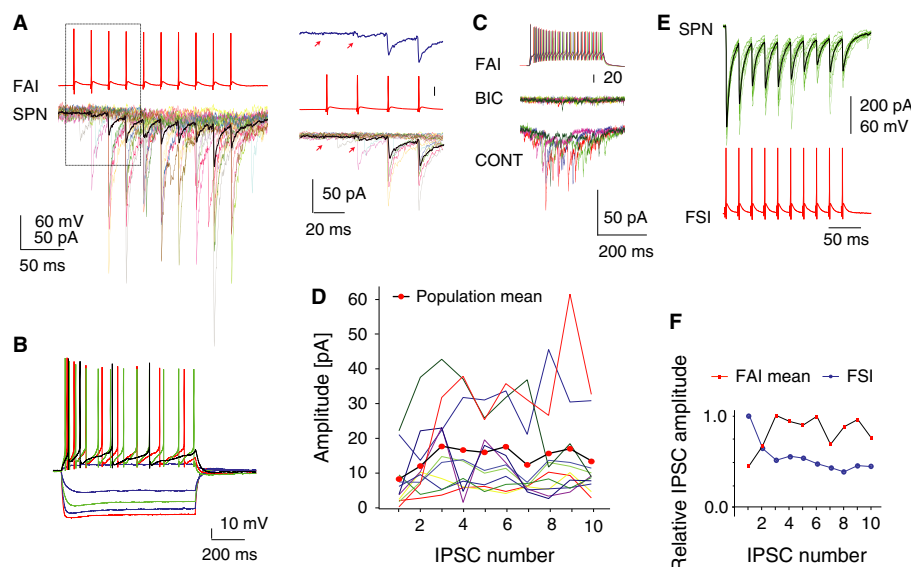

FIG. 3. Characterization of synaptic transmission between FAIs and SPNs. (A) IPSC trains in an SPN elicited by trains of presynaptic action potentials in an FAI; same cell as in B. The thick trace is the average, and thin traces are individual responses. Right panel shows the first four IPSCs at higher time resolution. Top trace is the average response. Note the failure of transmission at the first spike (arrows) and the pronounced facilitation of the response. (B) Membrane potential responses of the FAI recorded in A to injected current pulses. (C) The IPSCs elicited from an FAI are blocked by bicuculline (10 μM). (D) IPSC trains recorded in 11 FAI–SPN pairs. Thin lines are the average responses for each pair; the thick line is the population mean. Note the facilitation of the response through the first three IPSCs. (E) Paired recording from an FSI and an SPN. Same FSI as in Fig. 2A. Note the typical large-amplitude IPSCs, exhibiting a low failure rate and short-term depression (top panel). (F) Comparison of the normalized amplitudes of the population means of the IPSCs elicited from FAIs and the IPSCs recorded from the FSI–SPN pair shown in E. Note the different short-term dynamics of the two connections.

Finally, we obtained simultaneous recordings from six pairs of connected FAIs and SPNs in the double transgenic mice and directly confirmed that the same FAIs that could be activated by optogenetic stimulation of cholinergic inputs (Fig. 5C) also provided GABAergic innervation to SPNs (Fig. 5D).

Discussion

This study demonstrates the existence of a novel type of GABAergic interneuron in the neostriatum, the FAI, which receives strong nicotinic excitatory inputs and provides conventional fast GABAergic inhibitory inputs to SPNs.

FAIs represent a novel type of GABAergic interneuron in the neostriatum

There are several lines of evidence to support the contention that FAIs represent a novel class of interneurons in the neostriatum. First, these neurons could be clearly distinguished from FSIs, NPY-PLTS and NPY-NGF interneurons based on characteristics of their firing responses to somatically injected current pulses, the unique short-term facilitation of synaptic transmission from FAIs to SPNs, the kinetics of the IPSC and (in the case of NPY-PLTS) the absence of NOS expression in the Cre-expressing interneuron population (Figs 1 and 2). It is possible that FAIs represent one of the subtypes of the less extensively studied THINS, but the distinction of FAIs is supported by (i) specific firing and membrane potential responses to injected current pulses in THINS that are absent in FAIs, including depolarizing plateau potentials in Type I, II and III THINS and a rebound LTS at resting membrane potential in Type IV neurons; (ii) the absence of TH induction in the Cre-expressing cells, which is observed in a subset of THINS following 6-OHDA lesions of the nigrostriatal projection; and finally (iii) the absence of nicotinic EPSP/C in the subtypes of THINS (Types I and II) tested to date (Ibáñez-Sandoval *et al.*, 2010; Ünal *et al.*, 2013). FAIs could also be distinguished from other electrophysiologically novel interneurons based on the current–frequency relationships and other properties of these neurons, as discussed above. Although the differential expression of nicotinic receptor subunits suggests that FAIs might be further classified into subtypes, such a subdivision could not be confirmed by
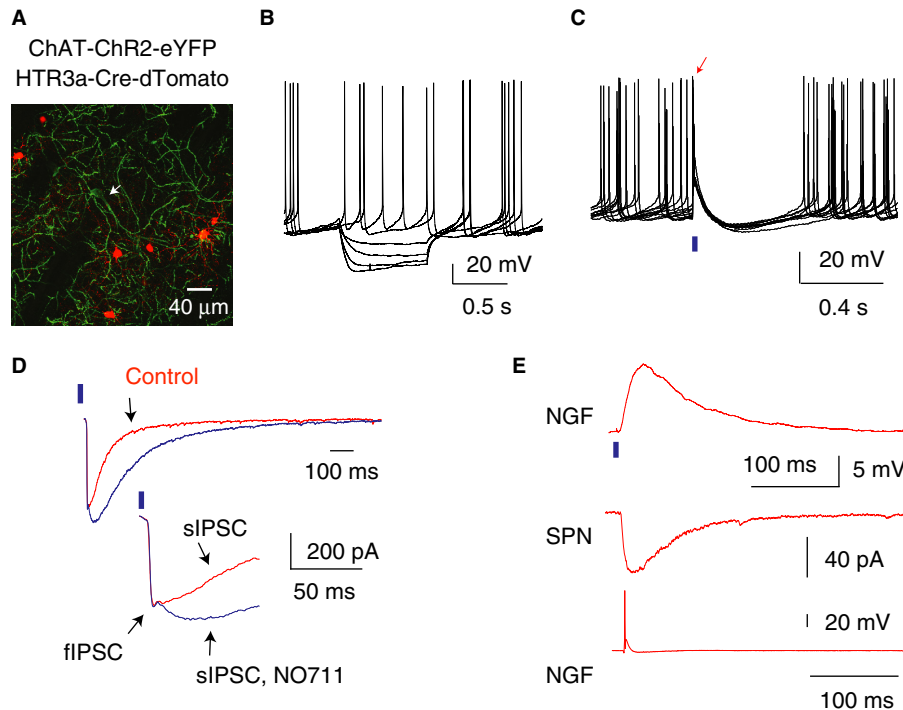
FIG. 4. Characterization of optogenetic responses in slices prepared from double transgenic *ChAT-ChR2-EYFP; HTR3a-Cre* mice. (A) Double transgenic visualization of cholinergic profiles with ChR2-eYFP and HTR3a-Cre interneurons with targeted expression of tdTomato (red) in double transgenic mice. The arrow points to a ChAT interneuron. Note the absence of colocalization of the two markers. (B) Voltage responses of a ChR2-EYFP-expressing ChAT interneuron to injected current pulses demonstrating typical electrophysiological properties of these cells, including spontaneous activity. (C) Brief light pulses (2 ms, blue bar) elicit single action potentials (arrow) and reset pacemaking in a spontaneously active ChAT interneuron. (D) Optogenetic activation of cholinergic interneurons and axons with 2-ms pulses of blue light (blue bars) elicits large-amplitude postsynaptic responses in an SPN, top and bottom traces. Note that application of the GABA transport blocker NO711 (10 μM) significantly increases the decay time constant of the late phase of the response (sIPSC). Also note that a relatively small, early fast component (fIPSC) was not affected by this drug. Inset shows the fIPSC–sIPSC transition at higher time resolution (bottom traces). (E) Top trace. Optogenetic stimulation (2-ms pulses of blue light, blue bar) elicited a large-amplitude EPSP in the HTR3a-Cre NPY-NGF interneuron. Same cell as in Fig. 2B. Paired recording from this neuron (bottom trace) and a nearby SPN (middle trace) demonstrates that the interneuron elicited a slow IPSC in the SPN (middle trace). Note that the intrinsic (Fig. 2B) and synaptic properties of the neuron are typical for NPY-NGF interneurons.

considering additional characteristics. Therefore, FAIs probably represent a distinct and novel cell type of the neostriatum.

In a recent study, Muñoz-Manchado *et al.* (2014) described several types of GABAergic interneurons targeted in HTR3a-EGFP transgenic mice. Surprisingly, despite nominally targeting the same neuron populations defined by the expression of the same gene, none of the cell types described in the HTR3a-EGFP line appears to match the properties of FAIs. In particular, among the neurons most similar to FAIs (the Type-III neurons of Muñoz-Manchado *et al.*, 2014) many were reported to exhibit a slow regenerative depolarizing potential that we never observed in FAIs or any other striatal interneurons targeted in the HTR3a-Cre line. Although the electrophysiological difference between FAIs and the heterogeneous Type-III neuron population may simply reflect different conditions of the recordings or preparations, or a difficulty of discerning FAIs in a different context of neuronal phenotypes, the fact that the two transgenic lines also diverge in their targeting of TH$^+$ interneurons confirms the existence of a genuine mismatch between the cell types accessible in the two transgenic lines and suggests that few or perhaps none of the FAIs are visualized in the HTR3a-EGFP mice.

FAIs are not a major source of the fIPSC elicited in SPNs by synchronous activation of cholinergic interneurons

Previous experiments have shown that synchronous cholinergic activation elicits disynaptic multiphasic GABAergic inhibition in SPNs

(English *et al.*, 2012; Nelson *et al.*, 2014). This phenomenon is of interest because activation of these GABAergic synaptic responses may be instrumental in transmitting the short-duration multi-phasic responses that ChAT interneurons exhibit during presentation of behaviorally salient stimuli. The cellular mechanism that mediates these GABAergic responses is not completely understood. As shown by English *et al.* (2012), at least two distinct sources are involved, one that gives rise to a conventional fast GABAergic IPSC (fIPSC) and another responsible for a slow, reuptake sensitive response (sIPSC, see Fig. 4D). In contrast to the sIPSC – a significant source of which has been identified as the NPY-NGF interneuron (English *et al.*, 2012) – the origin of the fast inhibitory component remains unclear. We have suggested that this component may be mediated by synaptic activation of one or more additional types of interneurons (English *et al.*, 2012). Recently, this explanation was called into question by results showing that both fast and slow inhibition of SPNs can be triggered by acetylcholine-induced GABA release from nigrostriatal terminals (Nelson *et al.*, 2014). Our present results directly demonstrate that there are interneurons in the striatum that elicit fast GABAergic IPSCs in SPNs and are activated by cholinergic inputs. Surprisingly, however, FAIs are unlikely to represent a major source of the cholinergically induced fIPSC observed in SPNs. This is because DHβE can fully block the disynaptic inhibition seen in SPNs but fails to block EPSPs or prevent firing of action potentials in most FAIs. We suggest that postsynaptic responses originating from FAIs that continue firing action potentials
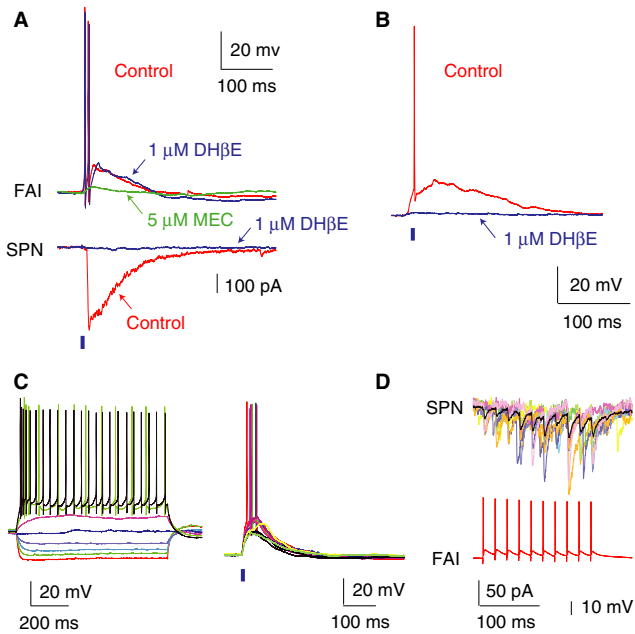
FIG. 5. Nicotinic cholinergic synaptic responses of FAIs. (A) Simultaneous recording from an FAI and an SPN. Optogenetic activation of cholinergic inputs (2-ms pulse of blue light, blue bar) elicited a large-amplitude IPSC in the SPN (bottom) and an EPSP giving rise to action potentials in the FAI (top). Application of DHβE (1 μM) had no significant effect on the EPSP or action potential firing in the FAI (top traces, arrow), but completely blocked the IPSC in the SPN (bottom traces, arrow). Subsequent application of MEC (5 μM) inhibited the EPSP in the FAI by ~80% (top traces, arrow). (B) Optogenetic activation of cholinergic inputs (2-ms pulse of blue light, blue bar) elicited an EPSP and the firing of an action potential in another FAI. The EPSP in this neuron was blocked by DHβE (1 μM, arrow). (C) Left panel: voltage responses to injected current pulses in a tdTomato-expressing HTR3a-Cre interneuron identified as an FAI. Right panel: optogenetic activation of cholinergic inputs (2-ms pulse of blue light, blue bar) elicited an EPSP and during some stimuli the firing of several action potentials in the same FAI. (D) Paired recording from the same FAI as in C and a nearby SPN demonstrated facilitating synaptic transmission to the SPN (top traces, think line is the average IPSC) in response to a presynaptic spike train (bottom trace).

in the presence of DHβE are not normally observed in most experiments due to the low amplitude and very low resting release probability of the response. Additionally, the low initial release probability and strong facilitation of the FAI to SPN synapse suggest that little inhibition is provided by FAIs during the first spike in a train, which would occur when the fIPSC is observed in SPNs.

The cellular origin of the fIPSC remains unclear. It is possible that most or perhaps all of this response originates from terminals of nigrostriatal axons as suggested by Nelson *et al.* (2014) although in their study despite using interventions that would be expected to eliminate neurotransmitter release from dopaminergic terminals, the block of the fIPSC was incomplete, suggesting that a significant fraction of this response component may originate from other, possibly intrinsic, interneuronal sources.

Implications for organization of the circuitry of the neostriatum

Our results reveal further complexity in the organization of the interneuron circuit of the neostriatum. Importantly, our results confirm that at least two types of GABAergic interneurons, NPY-NGF and FAI, that innervate SPNs are activated by excitatory cholinergic inputs in the neostriatum. We have previously shown that the

GABAergic interneurons responsible for recurrent inhibition in ChAT interneurons are distinct from those that give rise to the fIPSC or sIPSC in SPNs. As recurrent inhibition is fully blocked by low concentrations of DHβE (Sullivan *et al.*, 2008; English *et al.*, 2012), the majority of FAIs are not involved in this circuit. This suggests that at least three types of GABAergic interneurons receive nicotinic excitatory inputs in the neostriatum.

An interesting possibility is that some or all of the cholinergic input to FAIs originates from cholinergic neurons in the pedunculopontine nucleus (PPN) that are known to innervate the neostriatum (Dautan *et al.*, 2014) and the axons of which are probably activated during optogenetic experiments in slices prepared from ChAT-ChR2 mice. Although on quantitative grounds ChAT interneurons represent a more likely source of the cholinergic input than the significantly less dense input from the PPN (Dautan *et al.*, 2014), FAIs and perhaps other interneurons may be selectively targeted by the PPN projection, a notion supported by precedents for selective innervation of striatal interneurons by extrastriatal afferents (Bevan *et al.*, 1998; Brown *et al.*, 2012). It is further possible that the DHβE-sensitive and DHβE-insensitive cholinergic receptors are localized in an input-dependent manner as is the case for specific $GABA_A$ receptor subunits (Nyiri *et al.*, 2001; Gross *et al.*, 2011).

It is of significant interest that the cholinergic innervation of interneurons is cell type specific in the neostriatum. Rather than presenting a continuum of input strengths, the cholinergic innervation exhibits a high degree of selectivity contrasting with the complete or almost complete absence of nicotinic synaptic responses in FSIs and NPY-PLTS neurons (Ibáñez-Sandoval *et al.*, 2011; English *et al.*, 2012; Nelson *et al.*, 2014) with the extremely powerful innervation of NPY-NGF neurons (English *et al.*, 2012), FAIs and (based on indirect evidence) that of the still unidentified recurrent inhibitory interneurons (Sullivan *et al.*, 2008; English *et al.*, 2012). This suggests that the GABAergic interneurons that receive nicotinic inputs serve a fundamentally different role form other striatal GABAergic interneurons – one that is intimately linked to the cholinergic control of the striatum. Furthermore, these GABAergic interneurons appear to form a complex circuitry, as suggested by feed-forward slow inhibition elicited in NPY-NGFs by cholinergic stimulation, the electrotonic coupling of these neurons to each other (English *et al.*, 2012) and (based on their homology with cortical neurons) perhaps to other cell types (Simon *et al.*, 2005). Consequently, the neostriatum incorporates a more intricate and functionally diverse interneuronal circuitry than that which is usually assumed based on the canonical feed-forward organization of FSIs.

Possible significance for behavioral functions of acetylcholine

Cholinergic modulation is essential for the normal functioning of the neostriatum (Zackheim & Abercrombie, 2005; Pisani *et al.*, 2007; Bonsi *et al.*, 2011; Goldberg *et al.*, 2012). Recent experiments have revealed a powerful although not easily conceptualized role in learning for neostriatal ChAT interneurons (Sano *et al.*, 2003; Witten *et al.*, 2010; Brown *et al.*, 2012; Bradfield *et al.*, 2013; Okada *et al.*, 2014). Perhaps the most promising candidate to link cholinergic modulation to the regulation of learning is the brief multiphasic population response that ChAT interneurons exhibit in response to behaviorally salient stimuli. These responses consist of quickly alternating epochs of increased and reduced cholinergic activity, the precise pattern and magnitude of which reflect several learned characteristics of sensory stimuli (Aosaki *et al.*, 1994; Morris *et al.*, 2004; Atallah *et al.*, 2014). Recently,

several cellular responses (including those described here) have been identified that are sufficiently rapid to transmit these fast cholinergic signals and may have significant effects on excitatory synaptic plasticity (Pakhotin & Bracci, 2007; Ding *et al.*, 2010; Witten *et al.*, 2010; Cachope *et al.*, 2012; English *et al.*, 2012; Threlfell *et al.*, 2012). Among these, the control of GABAergic circuits by ChAT interneurons is a particularly attractive candidate because the rich integrative possibilities of networks of interneurons may provide a plausible interface for movement, attention and reinforcement-related mechanisms.

Acknowledgements

Abbreviations

AHP, afterhyperpolarization; CDS, coding sequence; ChAT, choline-acetyl-transferase-expressing; CR, calretinin; DHβE, dihydro-β-erythroidine; EPSP, excitatory postsynaptic potential; FAI, fast-adapting interneuron; FSI, fast-spiking interneuron; hGA, human growth hormone poly-adenylation; IPSC, inhibitory postsynaptic current; IQR, interquartile range; MEC, mecamylamine; NMDG, N-methyl-D-glucamine; NOS, nitric oxide synthase; NPY-NGF, neuropeptide-Y-expressing neurogliaform; PBS, phosphate-buffered saline; PLTS, plateau-depolarization low-threshold spiking; PV, parvalbumin; SPN, sympathetic preganglionic neuron; TH, tyrosine hydroxylase; THIN, TH-expressing interneuron; WPRE, woodchuck hepatitis post-transcriptional regulatory element.

References

Aosaki, T., Tsubokawa, H., Ishida, A., Watanabe, K., Graybiel, A.M. & Kimura, M. (1994) Responses of tonically active neurons in the primate's striatum undergo systematic changes during behavioral sensorimotor conditioning. *J. Neurosci.*, **14**, 3969–3984.

Atallah, H.E., McCool, A.D., Howe, M.W. & Graybiel, A.M. (2014) Neurons in the ventral striatum exhibit cell-type-specific representations of outcome during learning. *Neuron*, **82**, 1145–1156.

Bevan, M.D., Booth, P.A., Eaton, S.A. & Bolam, J.P. (1998) Selective innervation of neostriatal interneurons by a subclass of neuron in the globus pallidus of the rat. *J. Neurosci.*, **18**, 9438–9452.

Bonsi, P., Cuomo, D., Martella, G., Madeo, G., Schirinzi, T., Puglisi, F., Ponterio, G. & Pisani, A. (2011) Centrality of striatal cholinergic transmission in basal ganglia function. *Front. Neuroanat.*, **5**, 6.

Bradfield, L.A., Bertran-Gonzalez, J., Chieng, B. & Balleine, B.W. (2013) The thalamostriatal pathway and cholinergic control of goal-directed action: interlacing new with existing learning in the striatum. *Neuron*, **79**, 153–166.

Brown, M.T., Tan, K.R., O'Connor, E.C., Nikonenko, I., Muller, D. & Luscher, C. (2012) Ventral tegmental area GABA projections pause accumbal cholinergic interneurons to enhance associative learning. *Nature*, **492**, 452–456.

Cachope, R., Mateo, Y., Mathur, B.N., Irving, J., Wang, H.L., Morales, M., Lovinger, D.M. & Cheer, J.F. (2012) Selective activation of cholinergic interneurons enhances accumbal phasic dopamine release: setting the tone for reward processing. *Cell Rep.*, **2**, 33–41.

Dautan, D., Huerta-Ocampo, I., Witten, I.B., Deisseroth, K., Bolam, J.P., Gerdjikov, T. & Mena-Segovia, J. (2014) A major external source of cholinergic innervation of the striatum and nucleus accumbens originates in the brainstem. *J. Neurosci.*, **34**, 4509–4518.

Ding, J.B., Guzman, J.N., Peterson, J.D., Goldberg, J.A. & Surmeier, D.J. (2010) Thalamic gating of corticostriatal signaling by cholinergic interneurons. *Neuron*, **67**, 294–307.

English, D.F., Ibáñez-Sandoval, O., Stark, E., Tecuapetla, F., Buzsaki, G., Deisseroth, K., Tepper, J.M. & Koos, T. (2012) GABAergic circuits mediate the reinforcement-related signals of striatal cholinergic interneurons. *Nat. Neurosci.*, **15**, 123–130.

Gerfen, R.G., Paletzki, R. & Heintz, N. (2013) GENSAT BAC Cre-recombinase driver lines to study the functional organization of cerebral cortical and basal ganglia circuits. *Neuron*, **80**, 1368–1383.

Gertler, T.S., Chan, S. & Surmeier, D.J. (2008) Dichotomous anatomical properties of adult striatal medium spiny neurons. *J. Neurosci.*, **28**, 10814–10824.

Gittis, A.H., Nelson, A.B., Thwin, M.T., Palop, J.J. & Kreitzer, A.C. (2010) Distinct roles of GABAergic interneurons in the regulation of striatal output pathways. *J. Neurosci.*, **30**, 2223–2234.

Goldberg, J.A., Ding, J.B. & Surmeier, D.J. (2012) Muscarinic modulation of striatal function and circuitry. *Handb. Exp. Pharmacol.*, **208**, 223–241.

Grofova, I. (1974) The identification of striatal and pallidal neurons projecting to substantia nigra: an experimental study by means of retrograde axonal transport of horseradish peroxidase. *Brain Res.*, **91**, 286–291.

Gross, A., Sims, R.E., Swinny, J.D., Sieghart, W., Bolam, J.P. & Stanford, I.M. (2011) Differential localization of GABA$_A$ receptor subunits in relation to rat striatopallidal and pallidopallidal synapses. *Eur. J. Neurosci.*, **33**, 868–878.

Ibáñez-Sandoval, O., Tecuapetla, F., Unal, B., Shah, F., Koos, T. & Tepper, J.M. (2010) Electrophysiological and morphological characteristics and synaptic connectivity of tyrosine hydroxylase-expressing neurons in adult mouse striatum. *J. Neurosci.*, **30**, 6999–7016.

Ibáñez-Sandoval, O., Tecuapetla, F., Unal, B., Shah, F., Koos, T. & Tepper, J.M. (2011) A novel functionally distinct subtype of striatal neuropeptide Y interneuron. *J. Neurosci.*, **31**, 16757–16769.

Kawaguchi, Y. (1993) Physiological, morphological, and histochemical characterization of three classes of interneurons in rat neostriatum. *J. Neurosci.*, **13**, 4908–4923.

Kawaguchi, Y., Wilson, C.J., Augood, S.J. & Emson, P.C. (1995) Striatal interneurones: chemical, physiological and morphological characterization. *Trends Neurosci.*, **18**, 527–535.

Koos, T., Tepper, J.M. & Wilson, C.J. (2004) Comparison of IPSCs evoked by spiny and fast-spiking neurons in the neostriatum. *J. Neurosci.*, **24**, 7916–7922.

Lee, S., Hjerling-Leffler, J., Zagha, E., Fishell, G. & Rudy, B. (2010) The largest group of superficial neocortical GABAergic interneurons expresses ionotropic serotonin receptors. *J. Neurosci.*, **30**, 16796–16808.

Morris, G., Arkadir, D., Nevet, A., Vaadia, E. & Bergman, H. (2004) Coincident but distinct messages of midbrain dopamine and striatal tonically active neurons. *Neuron*, **43**, 133–143.

Muñoz-Manchado, A.B., Foldi, C., Szydlowski, S., Sjulson, L., Farries, M., Wilson, C., Silberberg, G. & Hjerling-Leffler, J. (2014) Novel striatal GABAergic interneurone populations labeled in the 5HT3aEGFP mouse. *Cereb. Cortex*, doi:10.1093/cercor/bhu179. [Epub ahead of print].

Nelson, A.B., Hammack, N., Yang, C.F., Shah, N.M., Seal, R.P. & Kreitzer, A.C. (2014) Striatal cholinergic interneurons drive GABA release from dopamine terminals. *Neuron*, **82**, 63–70.

Nisenbaum, E.S., Xu, Z.C. & Wilson, C.J. (1994) Contribution of a slowly inactivating potassium current to the transition to firing of neostriatal spiny projection neurons. *J. Neurophysiol.*, **71**, 1174–1189.

Nyiri, G., Freund, T.F. & Somogyi, P. (2001) Input-dependent synaptic targeting of alpha$_2$-subunit-containing GABA$_A$ receptors in synapses of hippocampal pyramidal cells of the rat. *Eur. J. Neurosci.*, **13**, 428–442.

Okada, K., Nishizawa, K., Fukabori, R., Kai, N., Shiota, A., Ueda, M., Tsutsui, Y., Sakata, S., Matsushita, N. & Kobayashi, K. (2014) Enhanced flexibility of place discrimination learning by targeting striatal cholinergic interneurons. *Nat. Commun.*, **5**, 3778.

Pakhotin, P. & Bracci, E. (2007) Cholinergic interneurons control the excitatory input to the striatum. *J. Neurosci.*, **27**, 391–400.

Pisani, A., Bernardi, G., Ding, J. & Surmeier, D.J. (2007) Re-emergence of striatal cholinergic interneurons in movement disorders. *Trends Neurosci.*, **30**, 545–553.

Sano, H., Yasoshima, Y., Matsushita, N., Kaneko, T., Kohno, K., Pastan, I. & Kobayashi, K. (2003) Conditional ablation of striatal neuronal types containing dopamine D2 receptor disturbs coordination of basal ganglia function. *J. Neurosci.*, **23**, 9078–9088.

Sciamanna, G. & Wilson, C.J. (2011) The ionic mechanism of gamma resonance in rat striatal fast-spiking neurons. *J. Neurophysiol.*, **106**, 2936–2949.

Simon, A., Olah, S., Molnar, G., Szabadics, J. & Tamas, G. (2005) Gap-junctional coupling between neurogliaform cells and various interneuron types in the neocortex. *J. Neurosci.*, **25**, 6278–6285.

Somogyi, P., Bolam, J.P. & Smith, A.D. (1981) Monosynaptic cortical input and local axon collaterals of identified striatonigral neurons. A light and

electron microscopic study using the Golgi-peroxidase transport-degeneration procedure. *J. Comp. Neurol.*, **195**, 567–584.

Sudweeks, S.N., Hooft, J.A. & Yakel, J.L. (2002) Serotonin 5-HT(3) receptors in rat CA1 hippocampal interneurons: functional and molecular characterization. *J. Physiol.*, **544**, 715–726.

Sullivan, M.A., Chen, H. & Morikawa, H. (2008) Recurrent inhibitory network among striatal cholinergic interneurons. *J. Neurosci.*, **28**, 8682–8690.

Taverna, S., Ilijic, E. & Surmeier, D.J. (2008) Recurrent collateral connections of striatal medium spiny neurons are disrupted in models of Parkinson's disease. *J. Neurosci.*, **28**, 5504–5512.

Tecuapetla, F., Koós, T., Tepper, J.M., Kabbani, N. & Yeckel, M.F. (2009) Differential dopaminergic modulation of neostriatal synaptic connections of striatopallidal axon collaterals. *J. Neurosci.*, **29**, 8977–8990.

Tepper, J.M., Tecuapetla, F., Koos, T. & Ibáñez-Sandoval, O. (2010) Heterogeneity and diversity of striatal GABAergic interneurons. *Front. Neuroanat.*, **4**, 150.

Threlfell, S., Lalic, T., Platt, N.J., Jennings, K.A., Deisseroth, K. & Cragg, S.J. (2012) Striatal dopamine release is triggered by synchronized activity in cholinergic interneurons. *Neuron*, **75**, 58–64.

Ünal, B., Shah, F., Kothari, J. & Tepper, J.M. (2013) Anatomical and electrophysiological changes in striatal TH interneurons after loss of the nigrostriatal dopaminergic pathway. *Brain Struct. Funct.*, **20**, 331–349.

Wilson, C.J. & Groves, P.M. (1980) Fine structure and synaptic connections of the common spiny neuron of the rat neostriatum: a study employing intracellular inject of horseradish peroxidase. *J. Comp. Neurol.*, **194**, 599–615.

Witten, I.B., Lin, S.C., Brodsky, M., Prakash, R., Diester, I., Anikeeva, P., Gradinaru, V., Ramakrishnan, C. & Deisseroth, K. (2010) Cholinergic interneurons control local circuit activity and cocaine conditioning. *Science*, **330**, 1677–1681.

Zackheim, J. & Abercrombie, E.D. (2005) Thalamic regulation of striatal acetylcholine efflux is both direct and indirect and qualitatively altered in the dopamine-depleted striatum. *Neuroscience*, **131**, 423–436.